

AD-A133 363

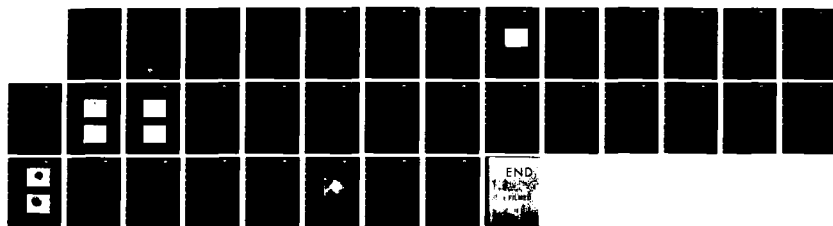
FIBER OPTIC LIGHT EMITTING DIODE(U) ROCKWELL  
INTERNATIONAL THOUSAND OAKS CA ELECTRONICS RESEARCH  
CENTER P D DAPKUS ET AL. AUG 80 ERC41025.15FR  
N66001-79-C-0209

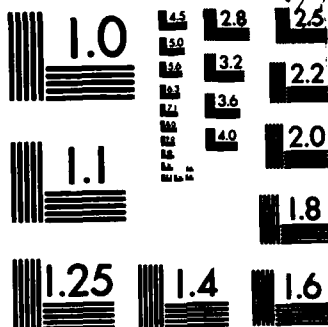
1/1

UNCLASSIFIED

F/G 20/6

NL





MICROCOPY RESOLUTION TEST CHART  
NATIONAL BUREAU OF STANDARDS-1963-A

AD-A133363

ERC41025.15FR

ERC41025.15FR

Copy No. \_\_\_\_\_

## FIBER OPTIC LIGHT EMITTING DIODE

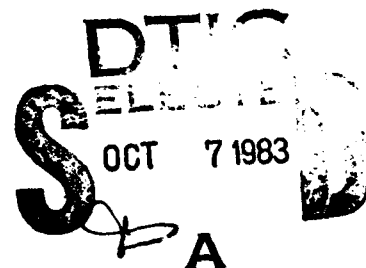
FINAL REPORT FOR THE PERIOD  
April 23, 1979 through August 1, 1980

GENERAL ORDER NO. 41025  
CONTRACT NO. N66001-79-C-0209

Prepared for

Naval Ocean Systems Center  
271 Catalina Blvd., Bldg. A-33  
San Diego, CA 92152

P. D. Dapkus  
Program Manager



AUGUST 1980

Approved for public release; distribution unlimited

DTIC FILE COPY



Rockwell International  
Electronics Research Center

83 09 19 081

**SECURITY CLASSIFICATION OF THIS PAGE (When Data Entered)**

(cont'd)

Unclassified

SECURITY CLASSIFICATION OF THIS PAGE(When Data Entered)

20. ABSTRACT

—> L.E.D.'s. The spectral width, near and far field of typical  $1.3\ \mu\text{m}$  GaInAsP/InP L.E.D.'s were measured. Finally, the modulation bandwidth and coupling efficiency of a packaged device into an optical fiber with a numerical aperture of 0.2 are presented. <

Unclassified

SECURITY CLASSIFICATION OF THIS PAGE(When Data Entered)



TABLE OF CONTENTS

|  | Page |
|--|------|
| 1.0 INTRODUCTION.....                                      | 1    |
| 2.0 QUATERNARY MATERIAL DEVELOPMENT.....                   | 1    |
| 2.1 GaInAsP/InP.....                                       | 1    |
| 2.2 GaAlAsSb/GaSb.....                                     | 2    |
| 3.0 DEVICE FABRICATION AND CHARACTERIZATION.....           | 8    |
| 3.1 Fabrication.....                                       | 8    |
| 3.2 Optical Output vs Driving Current.....                 | 12   |
| 3.3 Photoresponse, Spectral Width, Near and Far Field..... | 18   |
| 3.4 Modulation Bandwidth and Coupling Efficiency.....      | 22   |
| 4.0 CONCLUSION.....  | 26   |



|                    |                                     |
|--------------------|-------------------------------------|
| Accession For      |                                     |
| NTIS GRA&I         | <input checked="" type="checkbox"/> |
| DTIC TAB           | <input type="checkbox"/>            |
| Unannounced        | <input type="checkbox"/>            |
| Justification      |                                     |
| By                 |                                     |
| Distribution/      |                                     |
| Availability Codes |                                     |
| Availability       |                                     |
| Dist               | Special                             |
| A                  |                                     |



## 1.0 INTRODUCTION

The goal of this program was to develop light emitting diodes (LED) for optical communication at 1.27  $\mu\text{m}$  and 1.55  $\mu\text{m}$ , where present day optical fibers have the lowest loss and minimum dispersion. Double-heterostructure light emitting diodes from two quaternary systems, GaInAsP/InP and GaAlAsSb/GaSb were fabricated and compared.

Both quaternary systems, GaInAsP and GaAlAsSb, can be grown lattice matched to InP and GaSb substrates respectively. The GaInAsP quaternary system is a direct bandgap material between  $\sim (0.9 - 1.65) \mu\text{m}$ . As a result, low threshold current CW lasers<sup>(1)-(2)</sup> with long lifetimes have been demonstrated with this material system at 1.3  $\mu\text{m}$  as well as 1.55  $\mu\text{m}$ . By adding As to the GaAlSb ternary system, GaAlAsSb can be grown lattice matched to GaSb ( $\Delta a/a$  between AlSb and GaSb is only 0.7%). Avalanche photodiodes<sup>(3)</sup> with low dark current and high gain have been obtained with this material system in the same wavelength range. GaAlAsSb is, however, an indirect bandgap material in part of that wavelength range.

This report is divided into the following sections: Material Development, Device Fabrication and Characterization, and Conclusion.

## 2.0 MATERIAL DEVELOPMENT

### 2.1 GaInAsP Material Growth Development

Double heterostructure LED materials for 1.3  $\mu\text{m}$  were grown by liquid phase epitaxy at temperatures of approximately 650°C on both (100) and (111) oriented n-type InP substrates. The device structures consisted of a n-InP buffer layer grown on an InP substrate followed by a quaternary GaInAsP layer, a p-type InP confining layer, and a p<sup>+</sup> quaternary cap layer for ohmic contact purposes. The GaInAsP active layer, typically 0.5 to 1.0  $\mu\text{m}$  thick, was unintentionally doped with zinc owing to downward diffusion from the p-type InP layer during the growth process. Using electron beam induced current techniques, it was found that the amount of zinc used as the dopant in the p-InP confining



layer was critical to ensure the correct placement of the p-n junction at the GaInSP/InP heterointerface. Figure 1 shows a cleaved cross-section of a typical growth delineated by KOH: $K_3Fe(CN)_6$  etch. Good surface morphology was obtained on both (100) and (111) oriented substrates. The solidous compositions of the quaternary active layers were  $Ga_{0.23}In_{0.77}As_{0.48}P_{0.52}$  for (111) oriented substrates and  $Ga_{0.21}In_{0.79}As_{0.49}P_{0.51}$  for the (100) oriented substrates. The quaternary layers were grown at  $10^\circ$  supersaturation as determined by visual observation through the transparent furnaces.

The composition of the quaternary active layer of GaInAsP LEDs was expected to have a direct bearing not only on the emission wavelength but also on the lifetime and aging characteristics of the LEDs. In the latter case, the important characteristic is the degree of lattice matching to the InP substrates obtained in the quaternary layers. Work was undertaken to achieve a melt composition in which the quaternary layers were lattice matched exactly to the InP substrate. Both of these goals were achieved. Figure 2 shows the  $k_{\alpha 1}$  and  $k_{\alpha 2}$  reflection from the (400) plane of GaInAsP epitaxial layer grown on a (100) oriented InP substrate. The lattice mismatch for these two layers is found to be  $23.1 \times 10^{-4}$ . Other films on the (100) and the (111) substrates have been grown with the lattice mismatch of  $12 \times 10^{-4}$ . An important point to notice in the data of Fig. 2 is that the width of the intensity peaks is approximately 30 seconds, indicating that very little grading of the composition occurs during the growth of these thick quaternary layers. In fact, the width of these intensity peaks is limited by the resolution of the instrument.

Some efforts to grow GaInAsP/InP LEDs emitting at  $1.55 \mu m$  were undertaken in the last quarter. Although single quaternary layers with a bandgap corresponding to that wavelength were successfully grown (see monthly report #10), considerable difficulty was encountered during the growth of the p-InP confining layer on the quaternary active layer and the work was not completed.

## 2.2 GaAlAsSb Material Growth Development

The GaAlAsSb/GaAlSb light emitting diode materials with bandgaps corresponding to  $\sim 1.3 \mu m$  were initially grown at a temperature of  $525^\circ C$ . At this



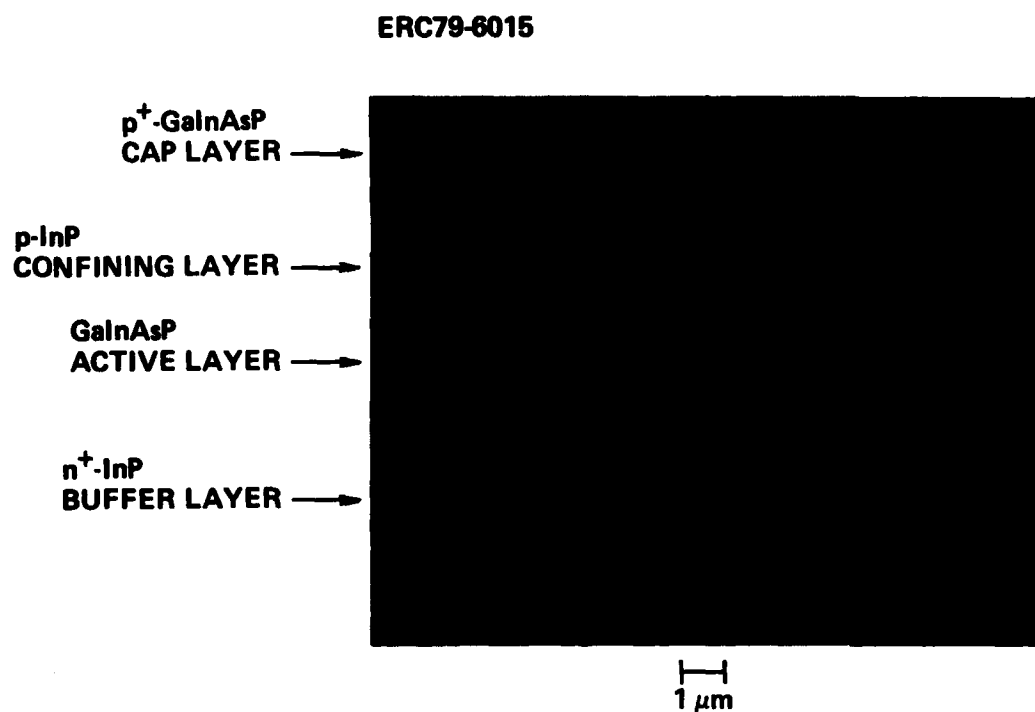


Fig. 1 Cleaved cross-section of a typical growth delineated by  $\text{KOH}:\text{K}_3\text{Fe}(\text{CN})_6$ .



SC79-5930

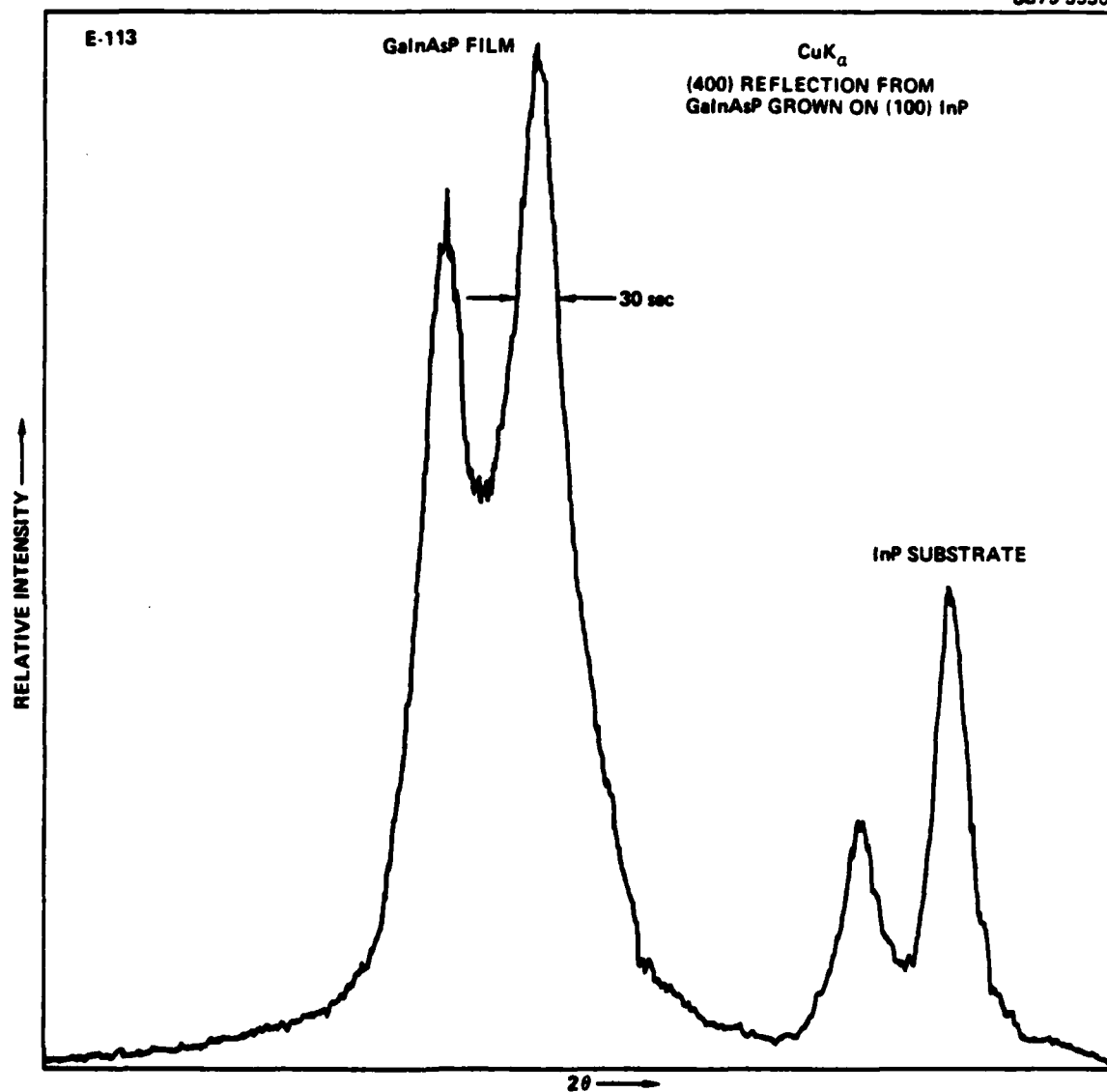


Fig. 2  $K_{\alpha 1}$  and  $K_{\alpha 2}$  reflection from the (400) plane of GaInAsP<sup>2</sup> epitaxial film grown on (100) InP.



low temperature, it is impossible to incorporate enough arsenic into the epitaxial layers to bring them to a lattice matched condition with GaSb substrate. However, the active layers and the confinement layers are lattice matched to one another. This is accomplished by the introduction of a buffer layer which also acts as one of the confining layers. All of the lattice mismatch between the substrate and the active layers is taken up in this buffer layer, and all subsequent layers are lattice matched to one another. The layers are grown in the following sequence. An  $n^+$  GaSb substrate ( $n \sim 7 \times 10^{17} \text{ cm}^{-3}$ ) was used as the substrate. An  $n^+$  confining layer of  $\text{Ga}_{0.6}\text{Al}_{0.4}\text{As}_{0.02}\text{Sb}_{0.98}$  was grown. This was followed by the active layer of  $\text{Ga}_{0.81}\text{Al}_{0.19}\text{Sb}$  (1.5  $\mu\text{m}$  thick). The active layer was unintentionally doped. The  $p^+$   $\text{Ga}_{0.6}\text{Al}_{0.4}\text{As}_{0.02}\text{Sb}_{0.98}$  confining layer was subsequently grown on top of the structure.

The quantum efficiency of light emitting diodes fabricated from epitaxial layers grown at the above temperature was found to be extremely low. It was speculated that the low quantum efficiency might be due to lattice mismatch between the active and confining layers. To achieve better matching, the quaternary GaAlAsSb layers were grown at temperatures higher than previously used. At 525°C, the arsenic incorporated in the Ga melt is not enough to achieve lattice matching with the GaSb substrate. Therefore, higher temperatures for the growth of this material were considered. At 550°C, the solubility of arsenic in Ga is substantially increased. The largest amount of arsenic incorporated into the quaternary at this temperature is 3.8%. This brings all of the layers of the LED structure close to lattice matching. Figure 3 shows the variation of the lattice constant with As composition in the melt. By comparing the quaternary layer and the corresponding ternary layer grown under the same conditions by double crystal X-ray diffractometry, we also found that the quaternary confining layers had a much narrower peak than the corresponding ternary layers (48 sec vs 5 min).

From photoresponse measurements, the bandgaps of the active layer in these double-heterostructures were found to be 0.95 eV, corresponding to a wavelength of  $\sim 1.3 \mu\text{m}$ . However, the quantum efficiencies of the LEDs subse

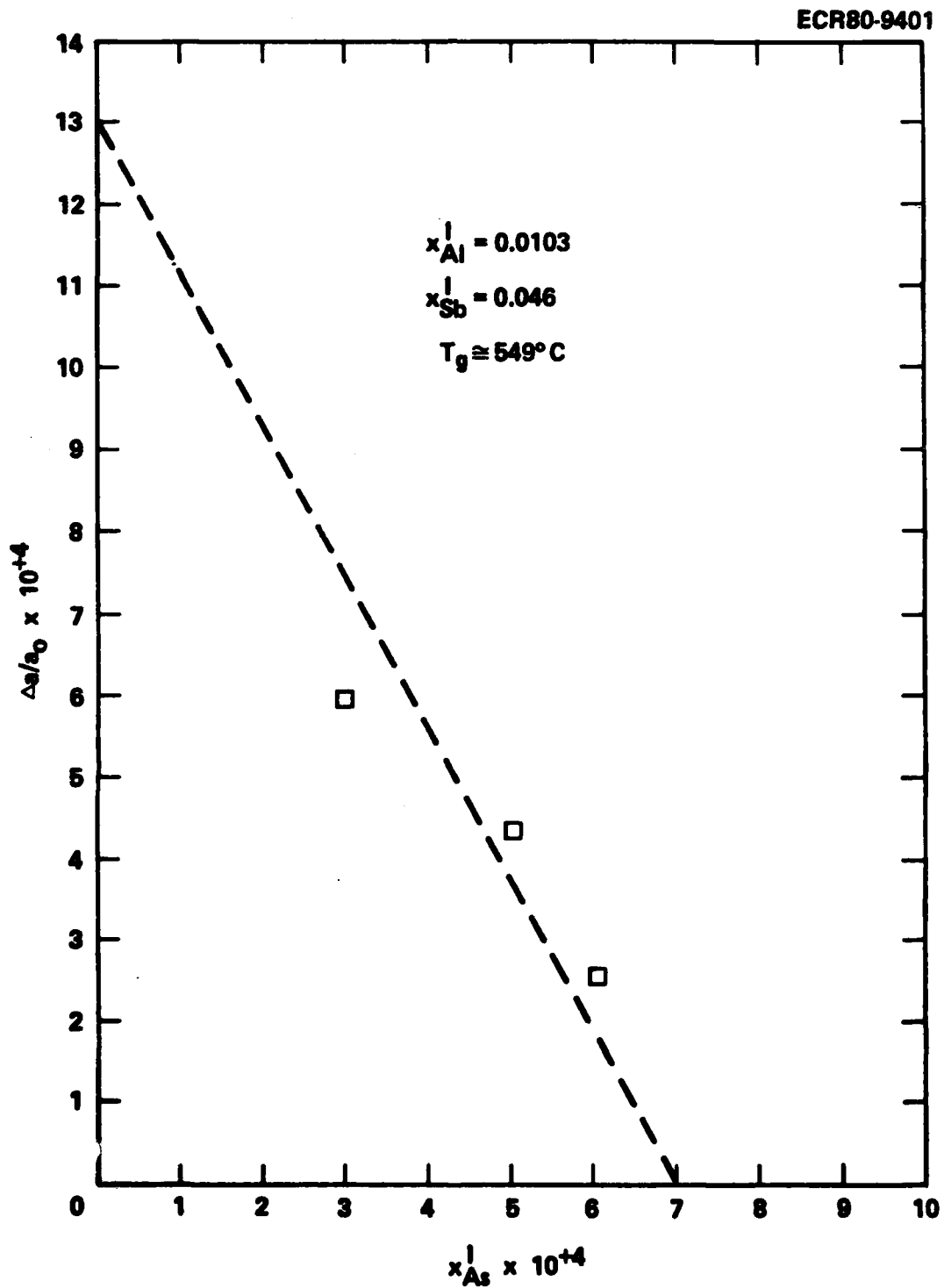


Fig. 3 Variation of the lattice mismatch of GaAlAsSb with As composition in the melt.



quently processed from these runs were found to be still rather low. A careful study of the separation between the direct conduction band minimum and indirect conduction band minimum in this material system indicated that the cross-over point between the two is near  $1.3 \mu\text{m}$ . A larger separation was expected at  $\sim 1.55 \mu\text{m}$ , at which wavelength the optical fiber has the lowest loss. As a result, efforts for this material system were directed towards the growth double-heterostructures emitting at  $1.55 \mu\text{m}$  during the last two quarters of the program. Devices of higher quantum efficiency were obtained as expected. The characterization of devices from both material systems will be described in the next section.



### 3.0 DEVICE FABRICATION AND CHARACTERIZATION

#### 3.1 Fabrication

Following growth by LPE, GaInAsP/InP wafers were processed into individual diodes. This was accomplished by the use of gold zinc and gold germanium contact metallization for the p and n-side, respectively. Contacts were made to the epitaxial side by opening windows through a SiO<sub>2</sub> mask. In the case of InP, light emitted by the quaternary active layer is not absorbed by the InP substrate. It was therefore extracted from the substrate side through contact openings. The device structure is shown in Fig. 4. Devices fabricated in the first quarter had contacts, 125  $\mu\text{m}$  and 250  $\mu\text{m}$  in diameter on the p-side and emission apertures 178  $\mu\text{m}$  and 285  $\mu\text{m}$  in diameter on the substrate side. To provide better matching between the LEDs and optical fibers with a typical diameter of 80  $\mu\text{m}$ , new mask sets were designed during the program. The diameter of the contact area on the p-side was reduced to be  $\sim 50$   $\mu\text{m}$ . Light was coupled from an emission aperture on the substrate side with a diameter of 90  $\mu\text{m}$ . The coupling efficiency between LEDs processed with the above mask set and fibers with a core diameter of  $\sim 80$   $\mu\text{m}$  will be given in Section 3.4. To reduce undesirable scattering from a rough surface, the substrate was polished before contact evaporation. The diodes were subsequently In-soldered p-side down to gold-plated headers. Using a quaternary cap layer, we were able to obtain series resistance as low as 1 ohm for devices with contact diameters of 50  $\mu\text{m}$ . This is to be compared with a typical series resistance of 5 ohms for devices with p-side contacts made directly on p-type InP confining layers. Typical I-V characteristic of an GaInAsP/InP LED with a contact diameter of 50  $\mu\text{m}$  is shown in Fig. 5.

The GaSb LEDs were mounted substrate side down on TO-5 headers. The contact on the p-side was in the form of a ring. The diameters of the emission area were 70  $\mu\text{m}$  and 115.7  $\mu\text{m}$ . The difficulty of achieving ohmic contact to n-GaSb was overcome during the program. Using Au-Sn as the contact metal for the n-side, series resistance of (4 - 10) $\Omega$  was obtained for devices with the above contact geometry (Fig. 6).



ERC41025.15FR

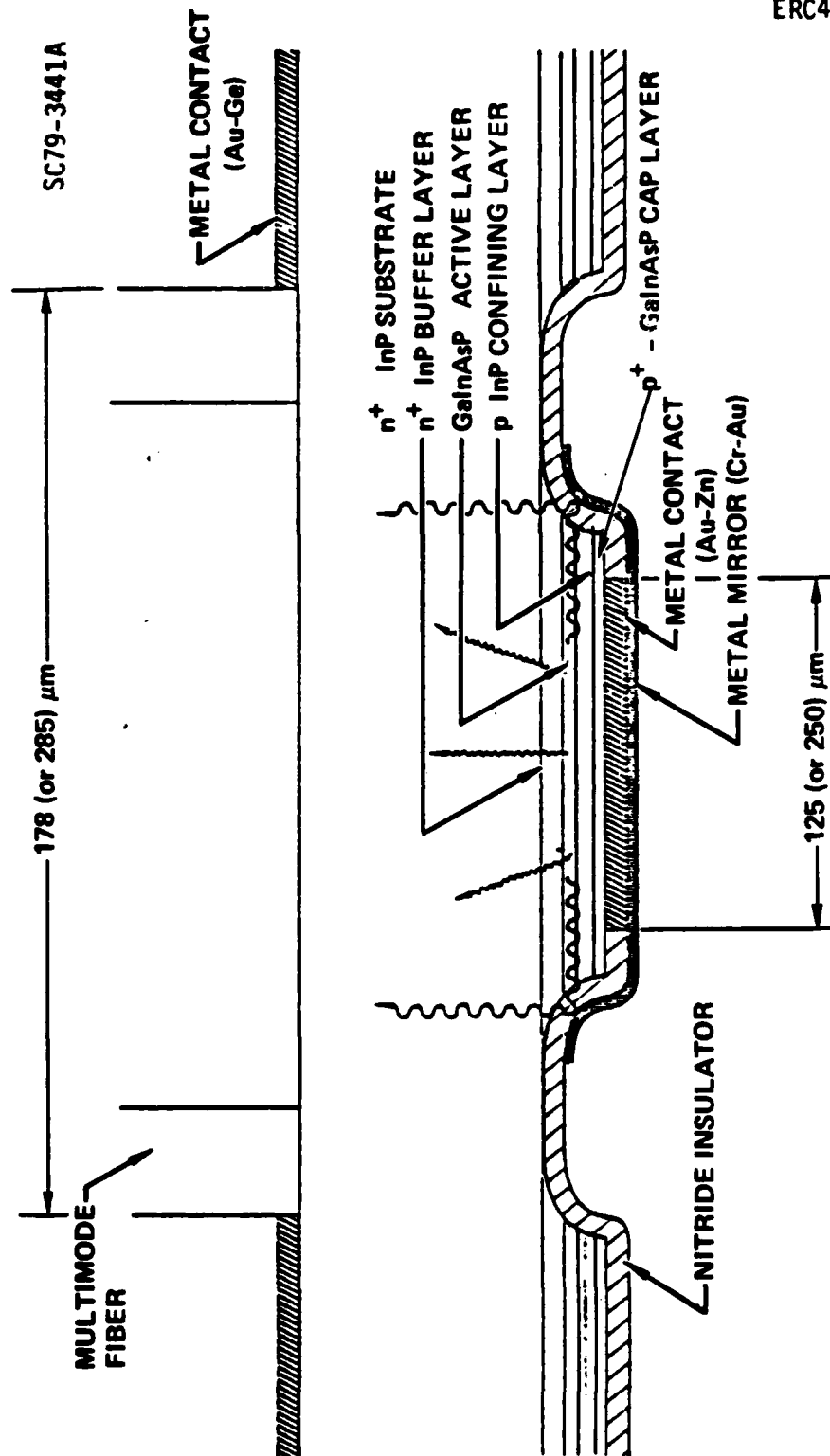


Fig. 4 Device structure of surface emitting GaInAsP/InP L.E.D.

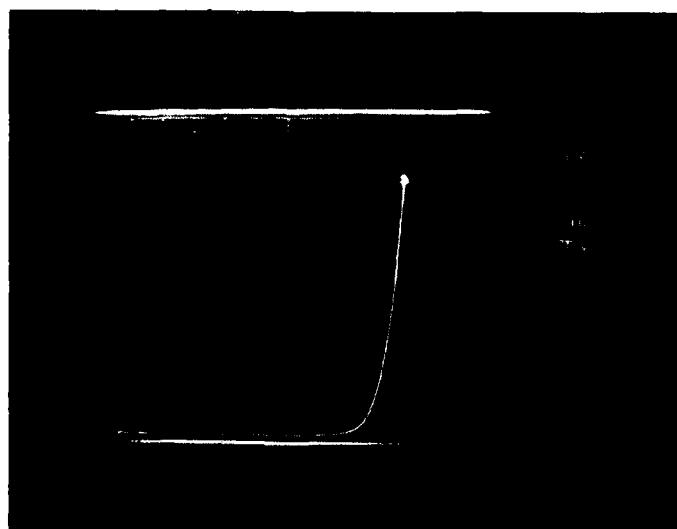
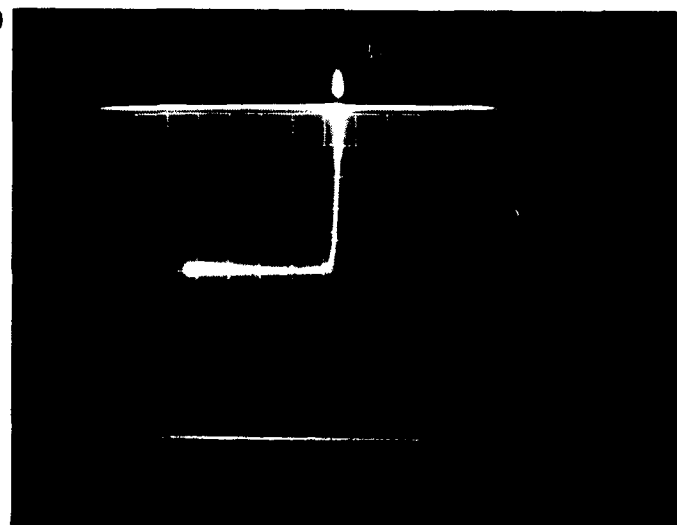


ERC41025.15FR

ERC80-9883

I-V CHARACTERISTICS OF  
GaInAsP/InP L.E.D.

H170



$r = 1 \Omega$

Fig. 5 Typical I-V characteristic of a GaInAsP/InP L.E.D.  
with a contact diameter of 50  $\mu\text{m}$ .



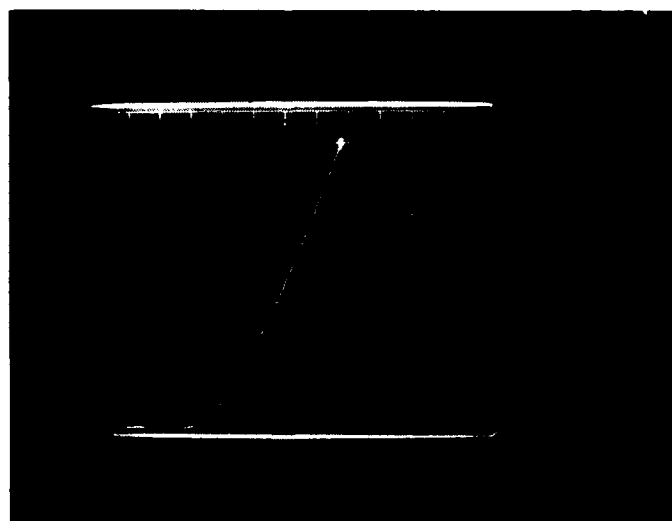
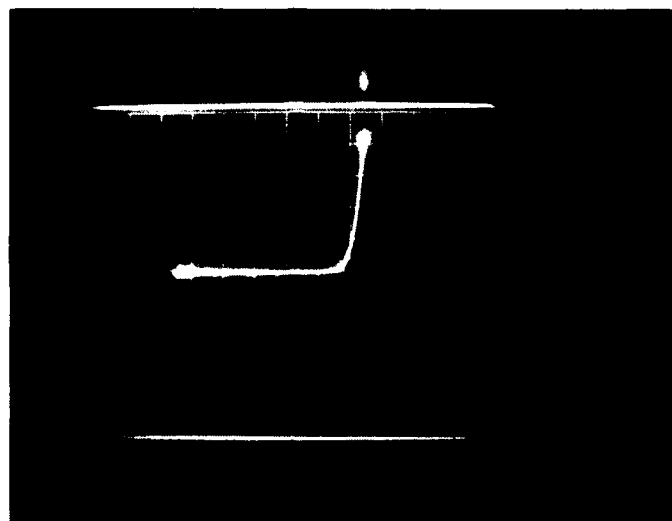


ERC41025.15FR

ERC80-9884

I-V CHARACTERISTICS OF  
GaAlAsSb/GaSb L.E.D.

J26



$r = 4\Omega$

Fig. 6 Typical I-V characteristic of a GaAlAsSb/GaSb L.E.D.



### 3.2 Optical Output vs Driving Current

After processing, the optical output from the LEDs was measured with a calibrated Ge detector. Figure 7 shows the typical output power from devices with contact diameters of 125  $\mu\text{m}$  (H134 and H139) and 50  $\mu\text{m}$  (H161) when they were driven at  $\sim 50\%$  duty cycle. For devices with a contact diameter of 125  $\mu\text{m}$ , the optical output varied linearly with driving current until  $\sim 200$  mA. The optical output usually saturates at  $\sim 800$  mA. The output power saturated at a lower driving current ( $\sim 400$  mA) when the contact diameter of the diode was reduced to 50  $\mu\text{m}$ . A quantum efficiency of 1 - 1.4% was obtained at 100 mA. Figure 8 shows the power output from a diode with a contact diameter of 125  $\mu\text{m}$  when driven at D.C. Approximately 1 mW was obtained at 100 mA. Thermal saturation limited the power output to  $\sim 1.8$  mW at higher DC currents.

Figure 9 shows a typical power output of the best batch of GaInAsP/InP LEDs. The diameter of the emission aperture was 90  $\mu\text{m}$ . A power output of up to 3.5 mW (at 400 mA) was obtained when the device was driven at  $\sim 50\%$  duty cycle. Proper alignment between the contact and emission area, as well as good heatsinking between the diode and the header are important considerations for maximizing the power output from these devices.

The optical output of the 1.3  $\mu\text{m}$  GaSb LEDs was typically three orders of magnitude below that of the InP LEDs. Quantum efficiencies of 0.01 - 0.05% were obtained for double-heterostructures LEDs from this material system with bandgaps corresponding to  $\sim 1.55$   $\mu\text{m}$ . Plots of the optical output versus driving current are shown in Fig. 10. The reason for the low quantum efficiency, even at wavelengths as long as 1.55  $\mu\text{m}$ , is believed to be the small separation between the direct and indirect conduction band. This is detailed below.

Figure 11 shows the band structure of GaAlSb as a function of the AlSb mole fraction in the solid.<sup>(4)</sup> The cross-over between the direct ( $\Gamma$ ) band and the indirect (L) band is at  $\sim 1.35$   $\mu\text{m}$ . Hence the range of wavelength in which the direct conduction band minimum is less than that of the indirect band is from  $\sim 1.8$   $\mu\text{m}$  (bandgap of GaSb) to  $\sim 1.35$   $\mu\text{m}$ . A salient feature of that plot is the small separation ( $\Delta E$ ) between the  $\Gamma$  and the L band, even for GaSb. The separation between the two at 1.8  $\mu\text{m}$  is  $\sim 0.085$  eV. This implies that a considerable

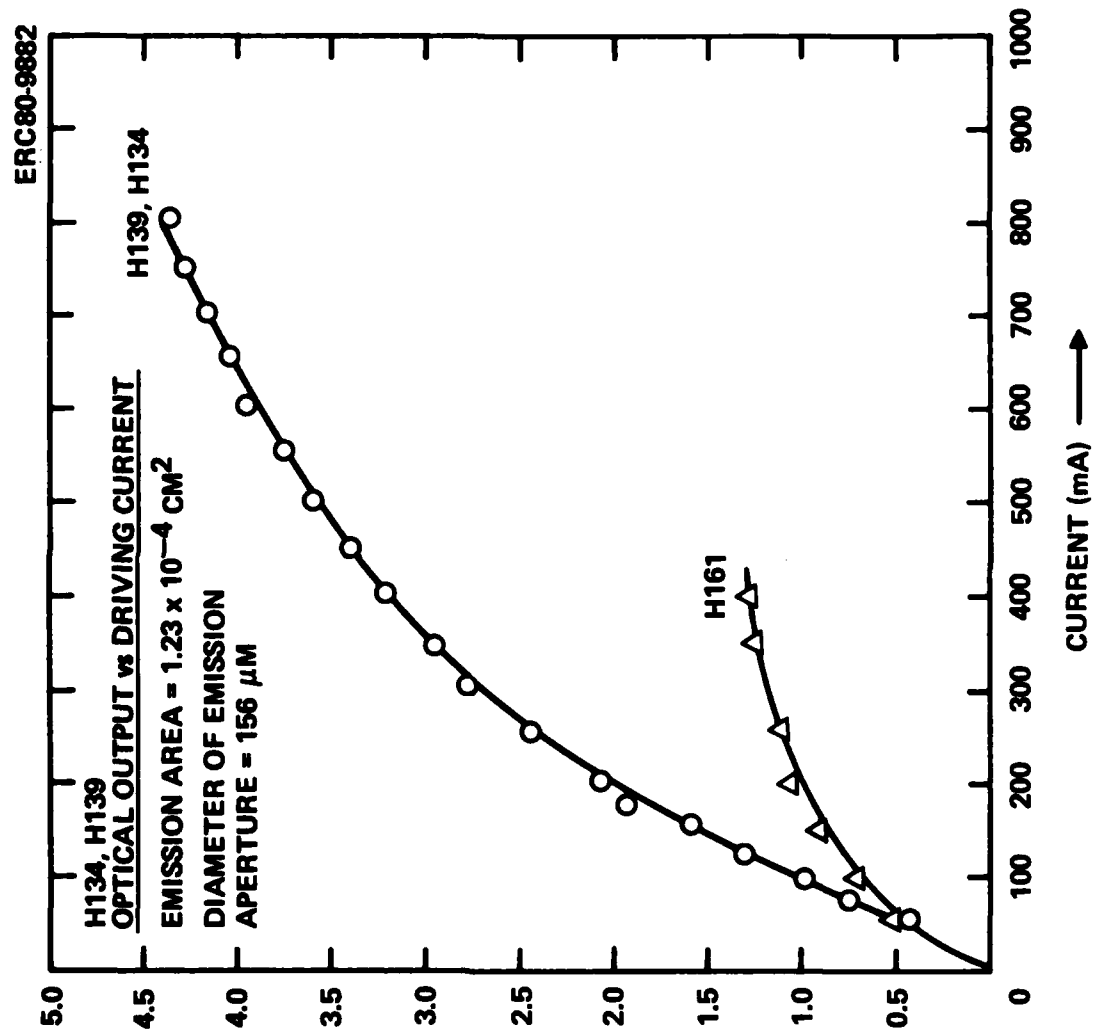


Fig. 7 Typical output power from devices with contact diameters of  $125 \mu\text{m}$  and  $50 \mu\text{m}$ .

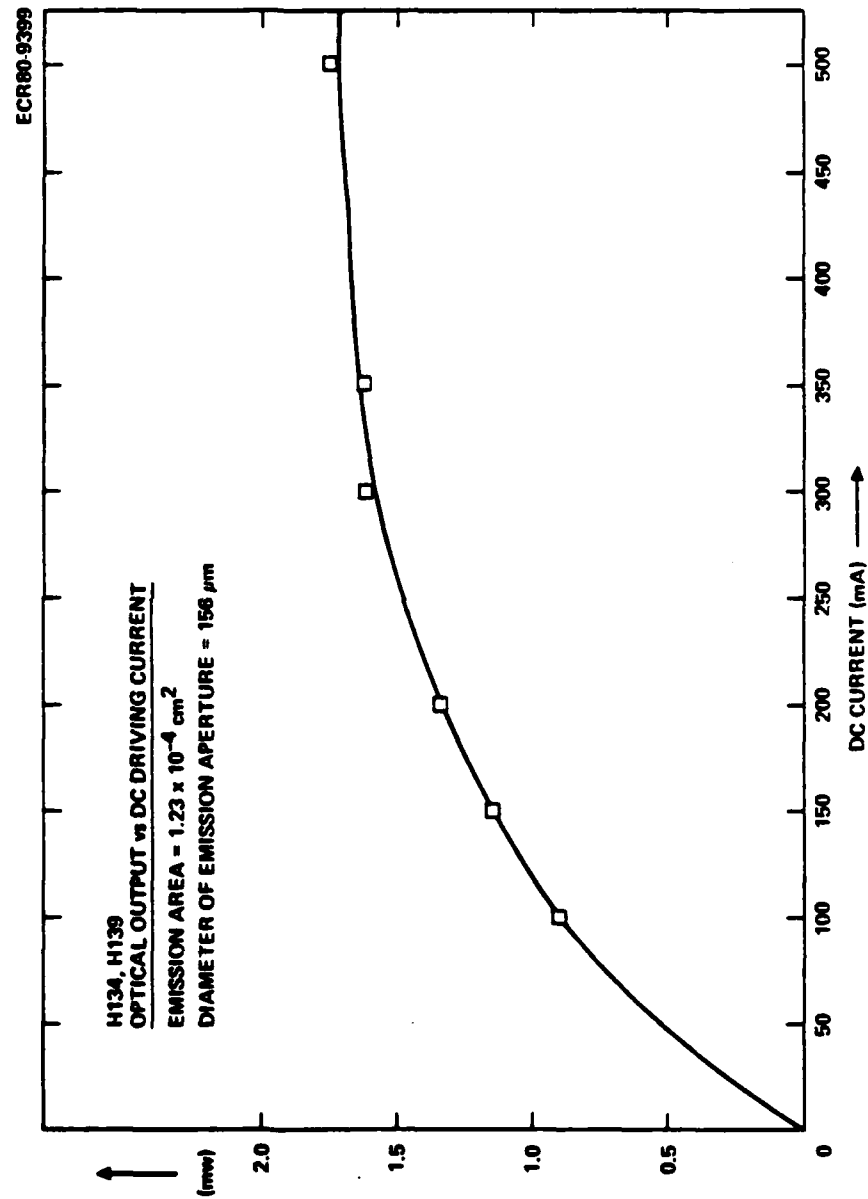


Fig. 8 DC output power from a diode with a contact diameter of  $125 \mu\text{m}$ .

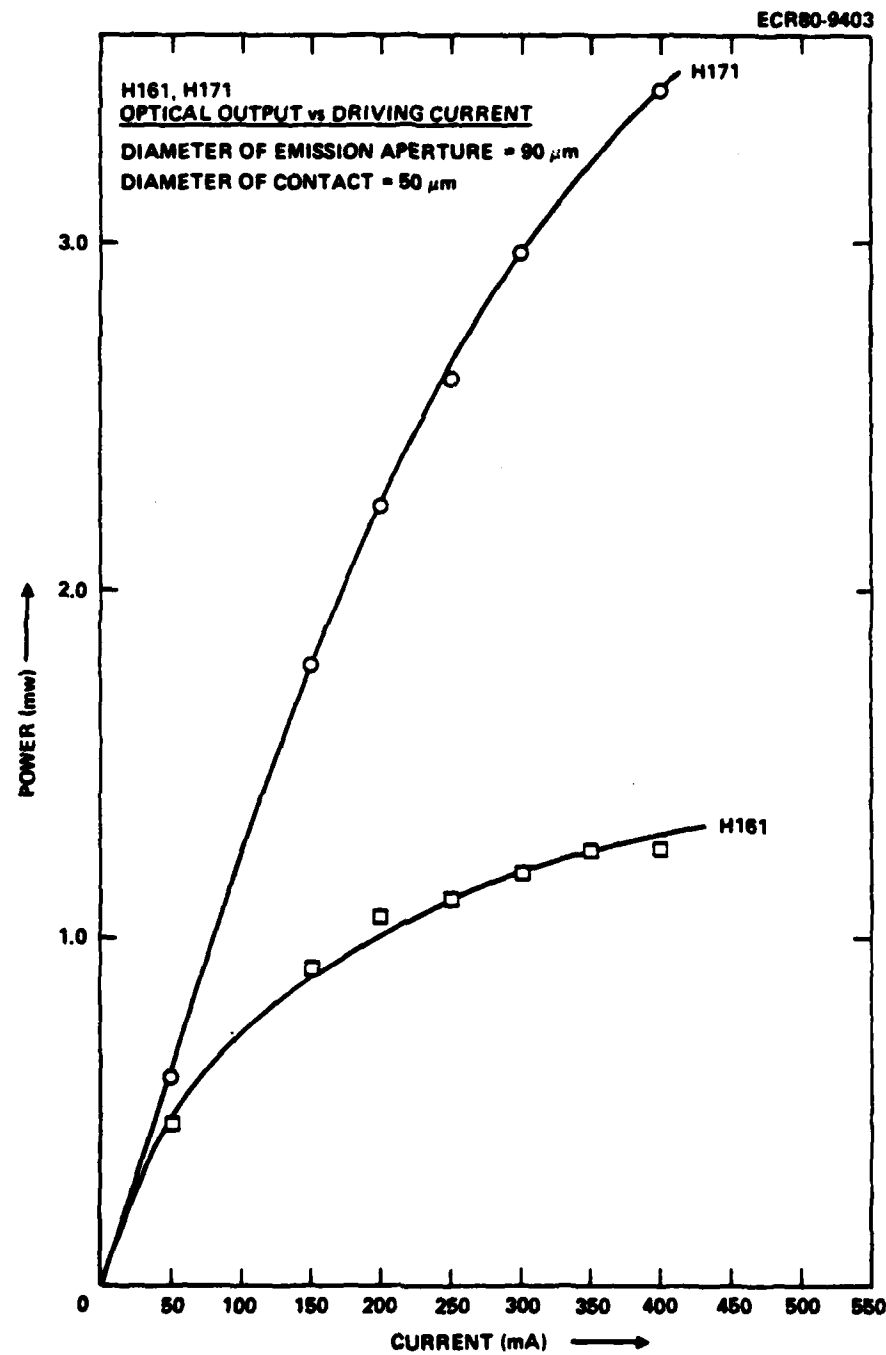


Fig. 9 Best results from 1.3  $\mu\text{m}$  GaInAsP/InP L.E.D.

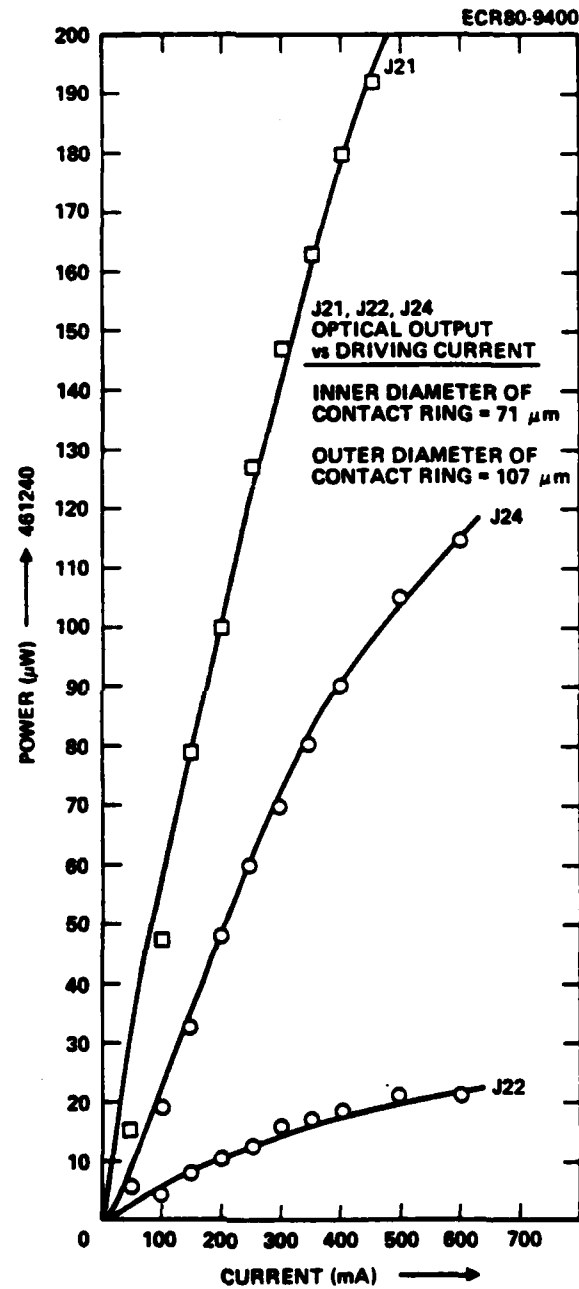


Fig. 10 Output power of GaSb L.E.D.



ERC41025.15FR

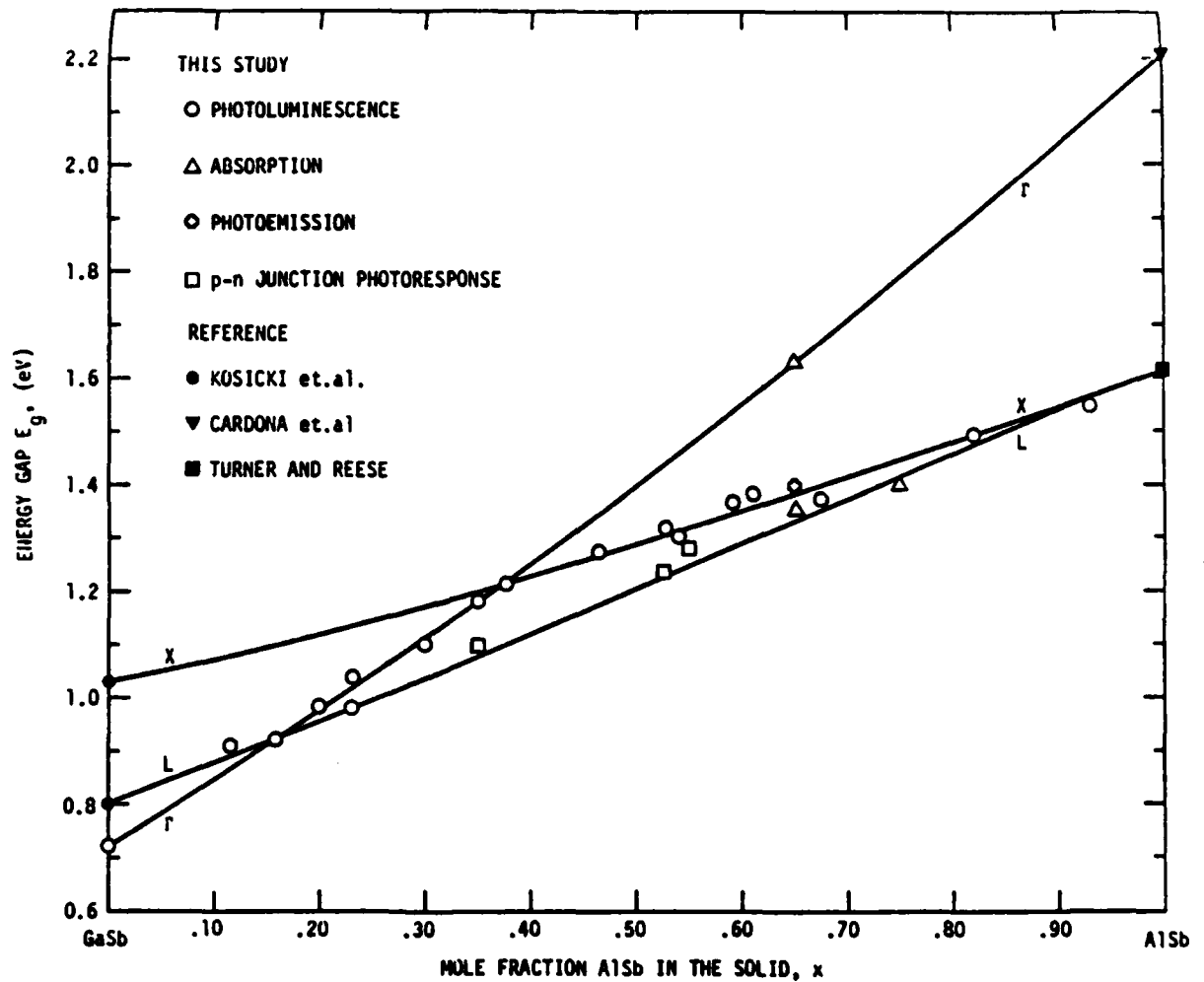


Fig. 11 Direct and indirect band structure of GaAlAsSb as a function of AlSb mole fraction in the solid.



number of electrons ( $n_2$ ) injected into the active layer "dwells" at the indirect conduction band at room temperature, from which radiative recombination is inefficient. The fraction ( $f$ ) of injected electrons that are capable of efficient radiative recombination is given by,<sup>(5)</sup>

$$f = \frac{n_1}{n_1 + n_2} = \frac{1}{1 + (N_2/N_1) \exp(-\Delta E/kT)} \quad (1)$$

where  $n_1$  and  $n_2$  are the electron concentrations in the direct and indirect minima, and  $N_2/N_1$  is the density of states ratio of the two bands. ( $N_2/N_1$ ) is proportional to  $(m_2^*/m_1^*)^{3/2}$ , where  $m_2^*$  and  $m_1^*$  are the density of states effective masses for the direct and the indirect minima respectively. Using a value of  $\sim 40$  for ( $N_2/N_1$ )<sup>(6)</sup> of GaSb,  $f$  is found to be  $\sim 0.4$  at room temperature ( $k = 0.026$  eV). This is to be compared with a fraction that is close to one for GaAs ( $\Delta E \sim 18.6$  kT at room temperature). Since the fraction of "radiative" electrons in the direct conduction band minimum is only 40% of those injected, the quantum efficiency of LEDs fabricated from the GaAlAsSb/GaSb quaternary system is lower than those fabricated from the GaInAsP/InP quaternary system.

### 3.3 Emission Spectrum, Near and Far Field

Emission spectrum of fabricated devices were measured with a lock-in amplifier and large area Ge detector. The emission spectrum of a GaInAsP/InP LED is shown in Fig. 12. The peak of the spontaneous emission was at  $\sim 1.27 \mu\text{m}$ . The full width at half maximum of the emission spectrum was  $\sim 800\text{\AA}$ , which meets the goals established for this program.

During the second quarter, a rotating table and infrared converter were set up for measuring the near and far field of the LEDs. The experimental set-up is shown in Fig. 13. The typical far field of a GaInAsP/InP LED is shown in Fig. 14. They were, as expected, approximately Lambertian with a half width of  $\sim 120^\circ$ .

Interesting features were revealed when the near field of the GaInAsP/InP LED was examined. The intensity distribution of these surface





ERC41025.15FR

SC79-6021

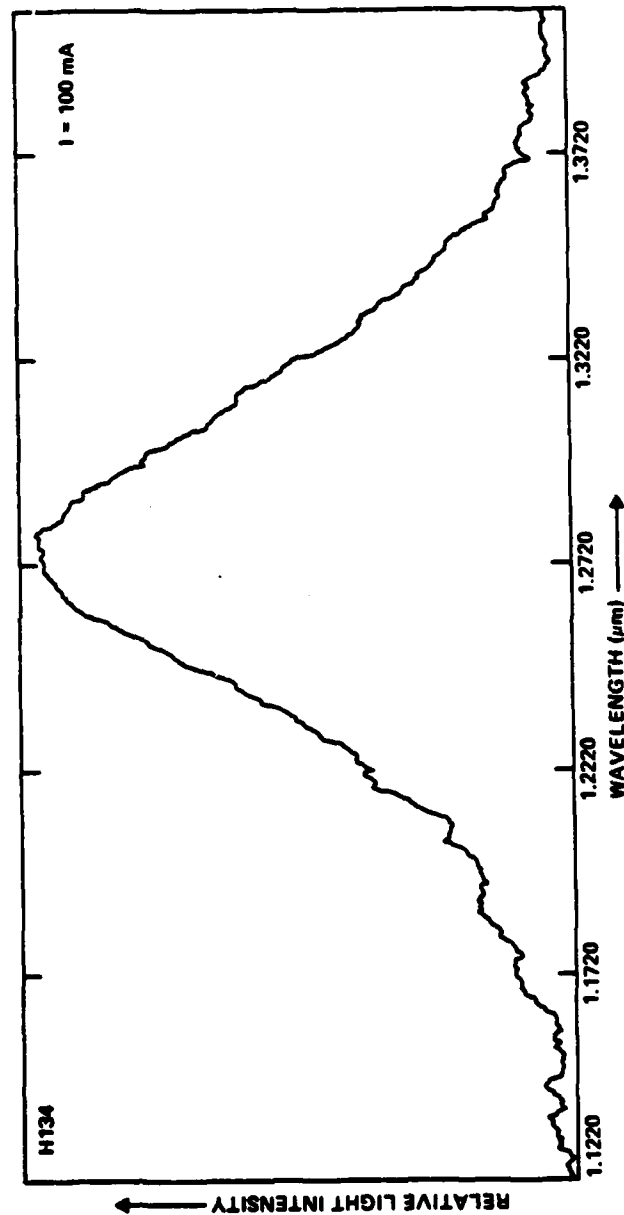


Fig. 12 Emission spectrum of GaInAsP/InP L.E.D.



SC80-10132

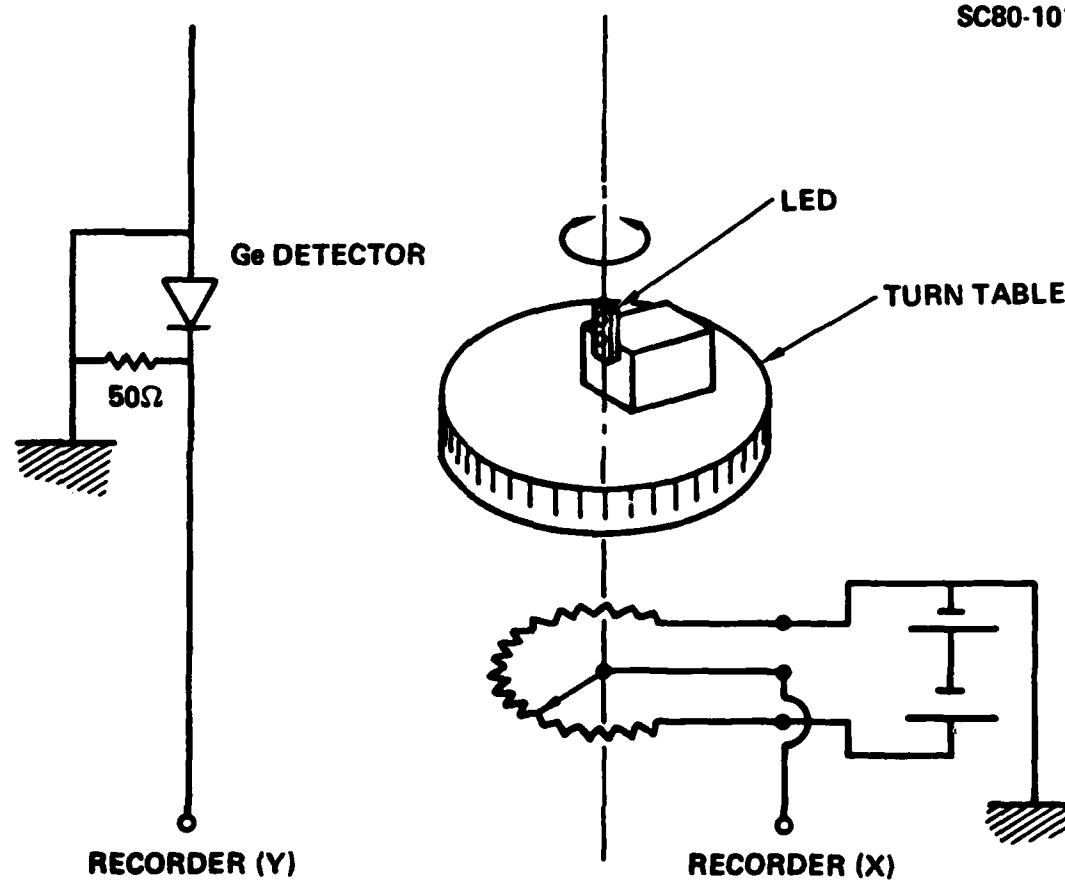


Fig. 13 Experimental set-up for far field measurement.



ERC41025.15FR

SC79-6001

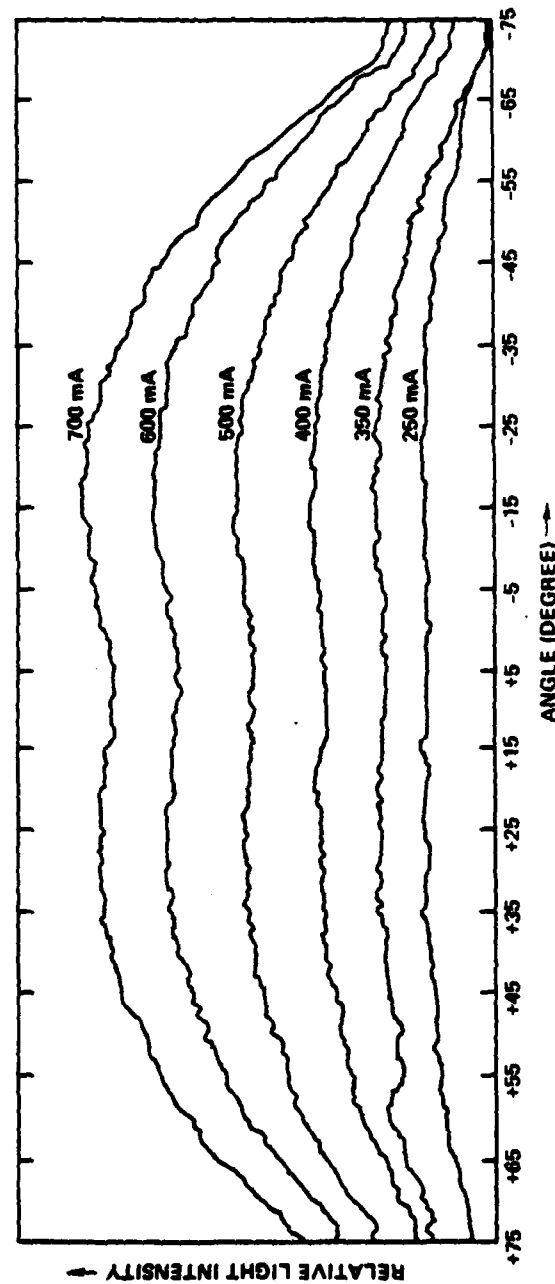


Fig. 14 Typical far-field of GaInAsP/InP L.E.D.



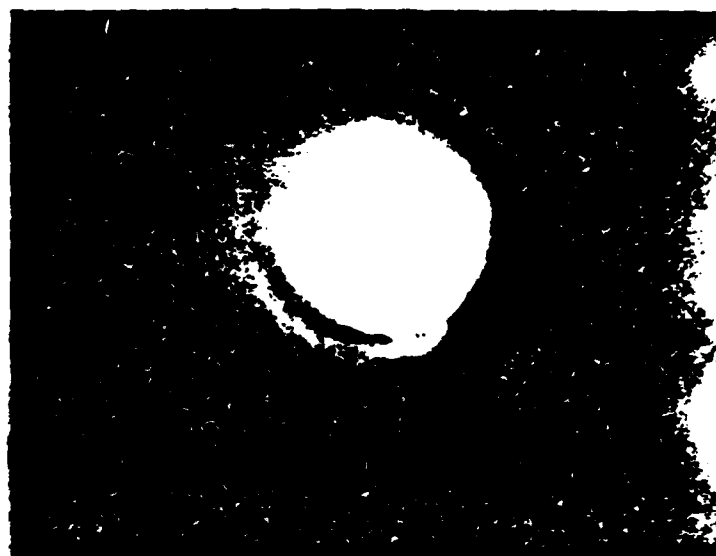
emitting LEDs was very uniform when the microscope was focused onto the emitting (substrate) surface (Fig. 15a). However, on focusing deeper into the device, dark lines in the form of cross-hatches appeared in the image (Fig. 15b). These "dark lines" are believed to originate from dislocations inherent in the (111)-oriented substrates.

The quantum efficiency of the GaAlAsSb/GaSb LED was too low for meaningful measurements of their spectral characteristics. However, the bandgap of the quaternary active layer can be easily determined from photoresponse measurements. The photoresponse of a GaAlAsSb/GaSb LED fabricated during the last quarter is shown in Fig. 16. The long wavelength cutoff of the photoresponse was determined by the bandgap of the quaternary active layer ( $\sim 1.55 \mu\text{m}$ ).

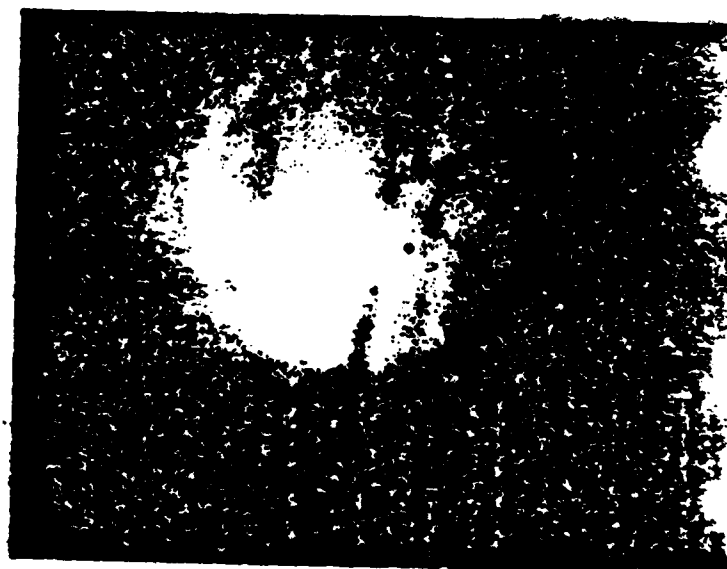
### 3.4 Modulation Bandwidth and Coupling Efficiency

During the last quarter, the coupling efficiency of the GaInAsP/InP LEDs into an optical fiber was measured. The emission apertures on the substrate side were  $90 \mu\text{m}$  in diameter. The optical fiber used had an inner core diameter of  $\sim 85 \mu\text{m}$  and a numerical aperture (N.A.) of  $\sim 0.2$ . After being mounted on fiber positioners on both ends, the optical fiber,  $\sim 260 \text{ cm}$ . in length, was butted against an LED at one end and a large area Ge-detector at the other end. The power coupled into the fiber, and the total power output of the LED is plotted in Fig. 17.

It is well known that the coupling efficiency ( $\eta_c$ ) from a Lambertian source such as a surface emitting LED into a step-index fiber is approximately given by the square of its numerical aperture. From our measurement,  $50 \mu\text{W}$  was coupled into the fiber at a driving current of  $110 \text{ mA}$ . This corresponded to a coupling efficiency of 4.5%, which is slightly higher than the estimated value of 4%. The difference between the two can be accounted for by the optical power carried by the fiber's "cladding-modes," which have been neglected for simplicity in the above estimation.



(a)



(b)

Fig. 15 Near field of GaInAsP/InP L.E.D.



ERC41025.15FR

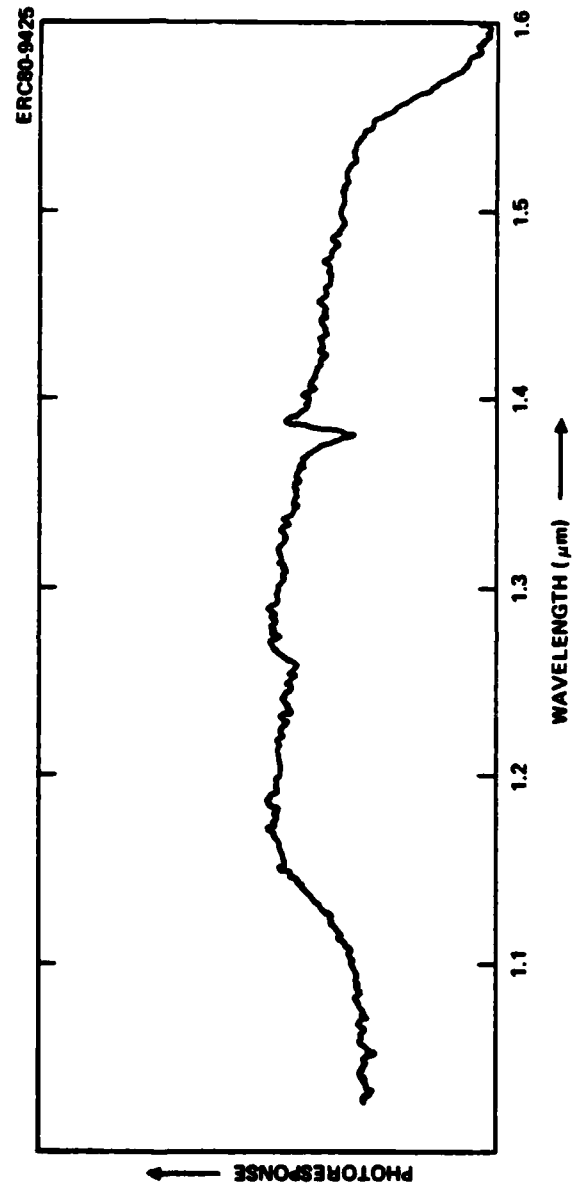


Fig. 16 Photoresponse of GaAlAsSb/GaSb L.E.D.

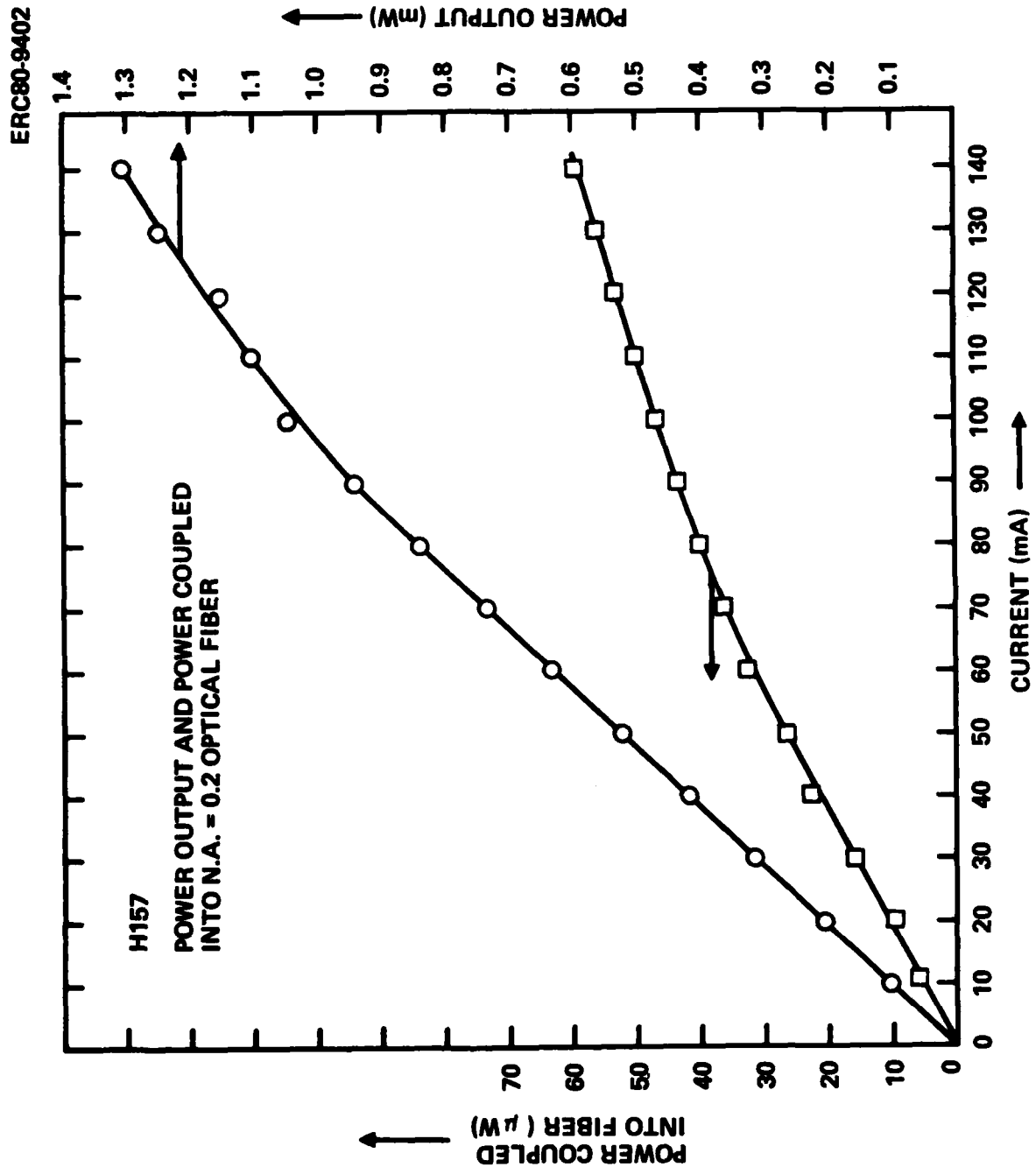


Fig. 17 Total output power and power coupled into optical fiber with N.A. of 0.2 from a typical GaInAsP/InP L.E.D.



A typical frequency response of the GaInAsP/InP LEDs is shown in Fig. 18. The diodes were modulated with 20 mA peak-to-peak r-f signal at bias current levels of 50 mA and 80 mA. The optical signal was detected with a fast GaAlAsSb/GaSb detector. As shown in the figure, the modulation bandwidths were 20 MHz and 25 MHz, respectively, at bias levels of 50 mA and 80 mA. The measured bandwidths were roughly proportional to the square root of the bias current, as we might expect from an estimation of the spontaneous emission lifetime under "large injection" conditions. The modulation bandwidth and coupling efficiency obtained above with the GaInAsP/InP LEDs therefore meet the goals set in the proposal for this program.

Eighty light emitting diodes (forty of each from the two material systems) was delivered at the end of the program. Their device characteristics correspond to those described in the above sections. A picture of one of the GaInAsP/InP LED, In soldered p-side down on a Au-plated heatsink, is shown in Fig. 19.

#### 4.0 CONCLUSION

Light emitting diodes were fabricated from two quaternary systems: GaInAsP/InP and GaAlAsSb/GaSb. Output power as high as 3.5 mW was obtained from the 1.27  $\mu\text{m}$  GaInAsP/InP LEDs when they were driven at  $\sim 50\%$  duty cycle. Their spectral width was typically  $\sim 800\text{\AA}$ . Approximately (50 - 80)  $\mu\text{W}$ , corresponding to a efficiency of  $\sim 40\%$ , was coupled into optical fibers with a numerical aperture of 0.2 and core diameter of  $\sim 90 \mu\text{m}$ . When biased at 80 mA, a modulation bandwidth of (25 - 30) MHz was obtained.

Figure 20 shows a plot of the fraction ( $f$ ) of electrons in the direct conduction band for the GaAlAsSb/GaSb material system as a function of  $\Delta E$ , the separation between the direct and indirect conduction band minima. Using Fig. 11,  $\Delta E$  can be related directly to the solid composition of GaAlAsSb, or the bandgap of the active layer. The same curve can be read as a plot of the relative quantum efficiency for these LEDs as a function of  $\Delta E$ . Our investigation shows that the small separation between the direct and indirect conduction band





ERC41025.15FR

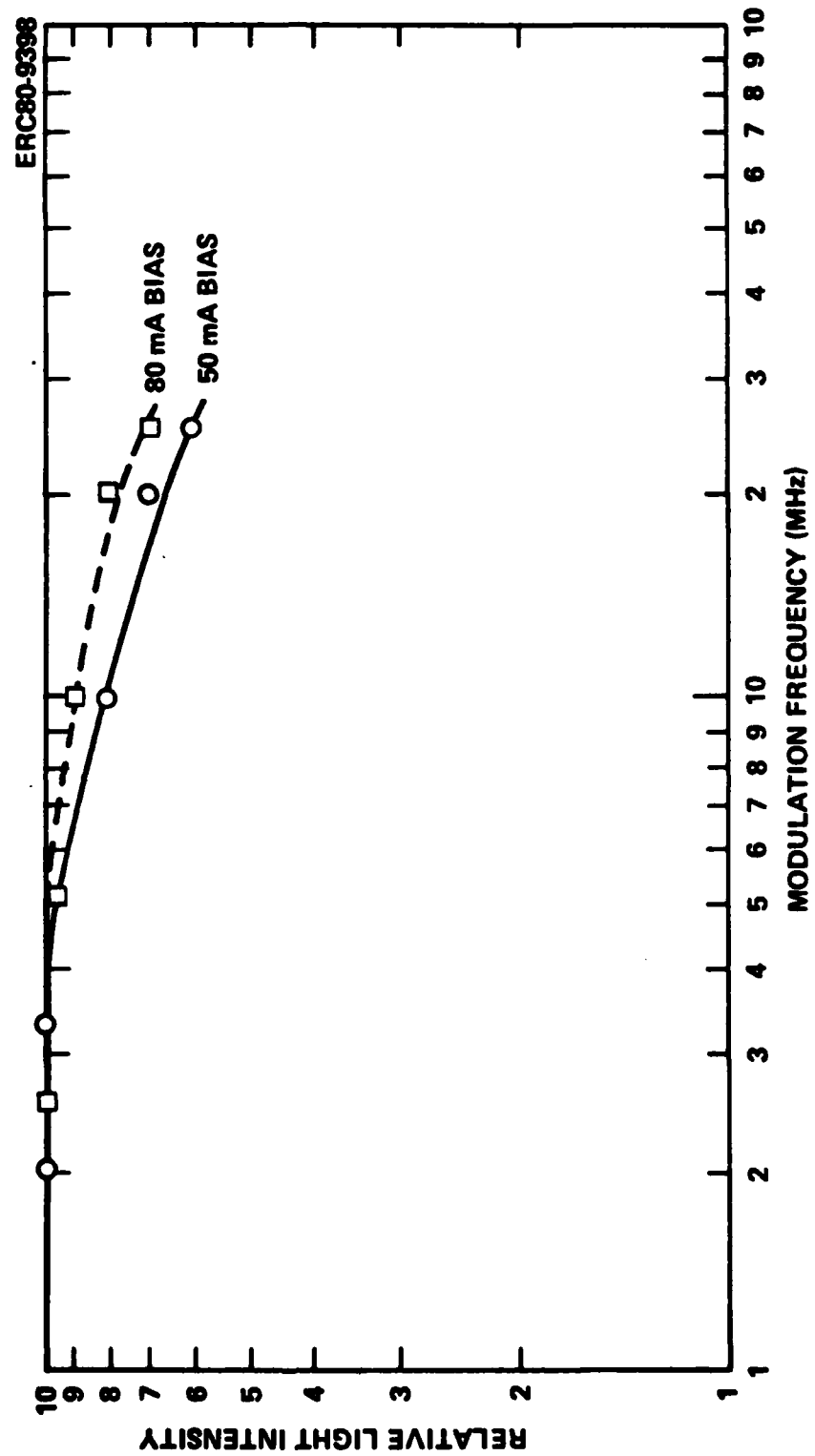


Fig. 18 Frequency response of GaInAsP/InP L.E.D.



ERC41025.15FR

ERC80-10133

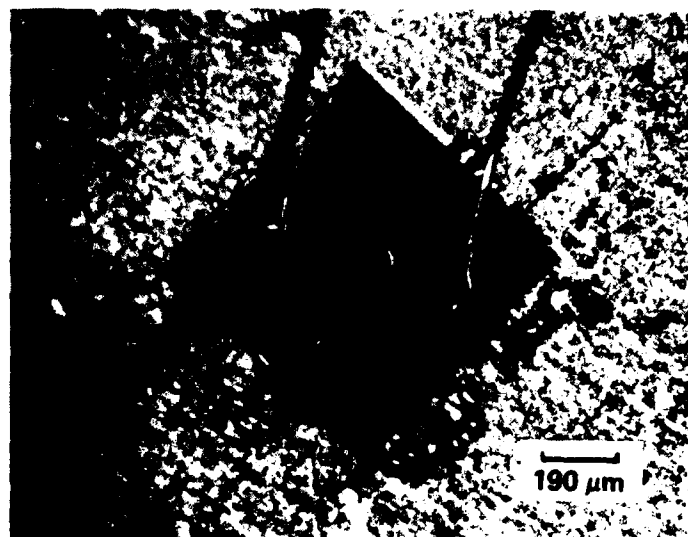


Fig. 19 A GaInAsP/InP L.E.D. In-soldered epi-side down in a header.

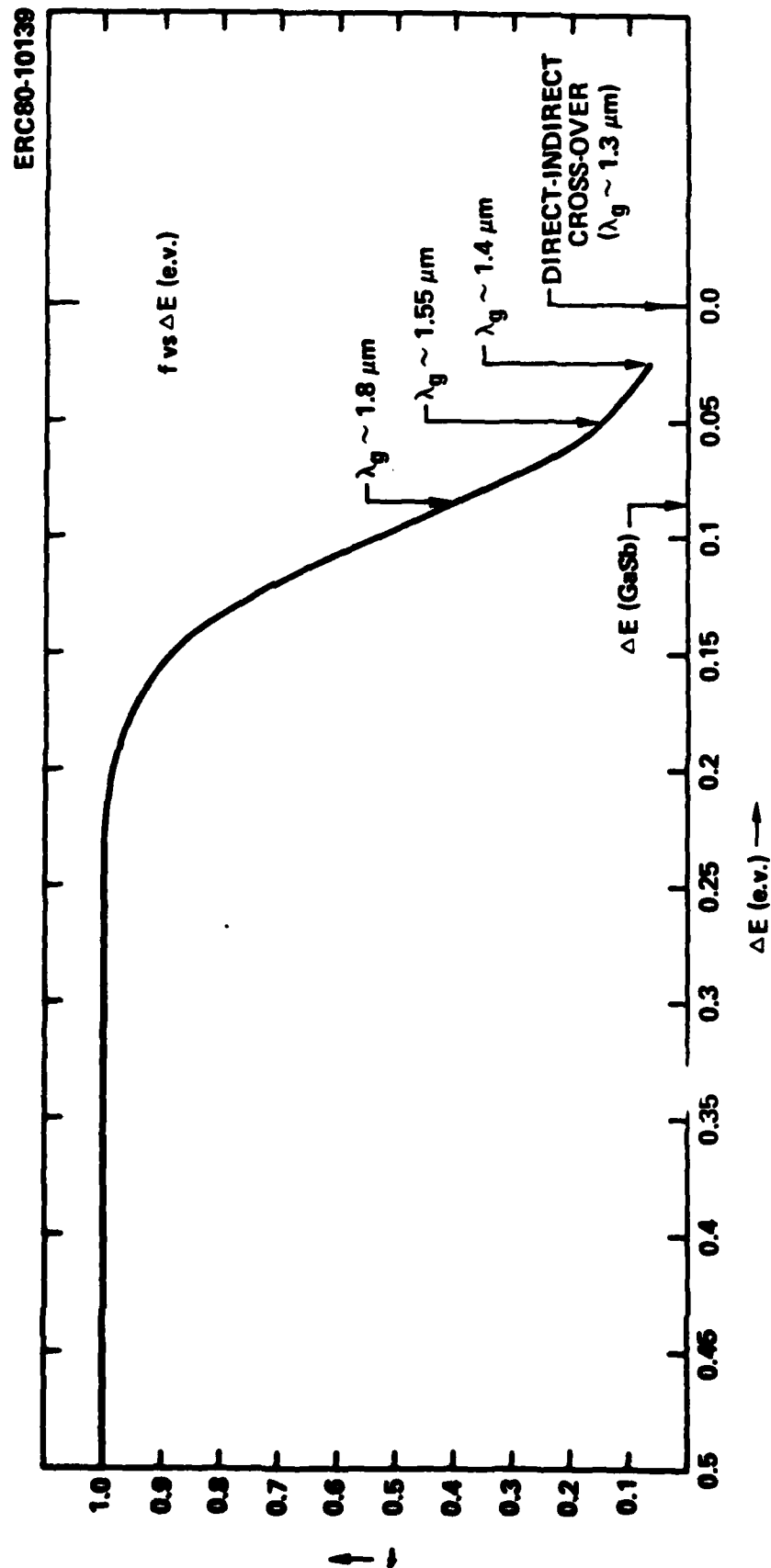


Fig. 20 Fraction  $f$  of electrons in the direct conduction band as a function of the separation between the direct and indirect conduction band minima.



minimum is the cause for the low quantum efficiency of the GaAlAsSb/GaSb LEDs. Compared with the GaInAsP/InP LEDs, for which  $\eta$  is close to 1, the curve shows that the quantum efficiency of the 1.55  $\mu\text{m}$  GaAlAsSb/GaSb should be less than 0.15 times that of the InP LEDs, which has a quantum efficiency of  $\sim 1 - 1.5\%$ . This is in good agreement with our experiment, in which a quantum efficiency of 0.05% was found for the GaAlAsSb/GaSb LEDs.

In conclusion, we found that the GaInAsP/InP LEDs have higher quantum efficiency than the GaAlAsSb/GaSb LEDs. The small separation between the L and  $\Gamma$  band of that material system is found to be the major cause for the low quantum efficiency observed.

#### REFERENCES

1. J.J. Hsieh, 1976 Appl. Phys. Lett. 28, 283.
2. W. Ng and P.D. Dapkus, to be published in IEEE J. of Quantum Electronics, Special Issue on Quaternary Material and Devices.
3. H.D. Law, J.S. Harris, K.C. Wong and L.R. Tomasetta, Inst. Phys. Conf. Ser. No. 45: Chapter 5, p. 420.
4. S.J. Anderson, F. Scholl, and J.S. Harris, Inst. Phys. Conf. Ser., No. 336, 1977, Chapter 6.
5. M.G. Craford, Prog. Solid State Chem. 8, 127 (1973)
6. B.B. Kosick, A. Jayaraman and W. Paul, Phys. Review, Vol. 172, No. 3, p. 172, 1968.

